**Journal of Engineering and Sustainable Development**
Vol. 30, No. 03, May 2026
https://jeasd.uomustansiriyah.edu.iq/index.php/jeasd
ISSN 2520-0917
**Research Article**
https://doi.org/10.31272/jeasd.2594

# Improving the Productivity of a Solar Still with the Aid of a Parabolic Trough Collector

Lujain S. Hyal*, Jalal M. Jalil, Abduljabbar O. Hanfesh

Electromechanical Engineering College, University of Technology, Baghdad, Iraq

*Email: lugain.s.hyal@uotechnology.edu.iq

**Article Info**

**Received** 17/04/2024
**Revised** 02/04/2026
**Accepted** 15/04/2026

**Abstract**

Water scarcity is mostly experienced within most parts of the world; This calls for the design of a portable, self-contained, low-cost desalination unit that can be used easily in an emergency or water shortages. This work is aimed at improving the performance of a single slope solar still. This research work is novel due to the direct coupling of the solar still unit with the parabolic concentrator, without any heat exchanger or PCM. Major conclusions of the test include that the productivity of the solar still is increased enormously once the PTC is integrated. The productivity improvements were measured at 13.5%, 34.3%, 66.5%, and 95.8% for flow rates of 0.004 kg/s, 0.001 kg/s, 0.0007 kg/s, and 0.0002 kg/s, respectively, when compared to a standard solar still. Efficiencies also demonstrated improvements with an increase in productivity. A further analysis revealed that the cost of water produced was approximately $ 0.053/liter for the conventional solar still, while the modified system was at an approximate $ 0.036/ liter. The overall inferences drawn from this research highlighted that the PTC technology can substantially improve productivity and efficiency in a solar still, making it more feasible in combating the water scarcity problem in resource-poor regions.

**Keywords:** Basin liner, Brackish water desalination, Hourly yield, Solar desalination, Productivity.

## 1. Introduction

Water is vital for the irrigation of crops and functions as a primary supply of potable water for rural regions. However, the majority of the water sources currently available are unsuitable for drinking due to their high levels of salt and pollution. Environmental pollution and energy supply are two of the most significant issues facing people globally. Different desalination techniques, such as filtration and distillation, are employed to purify saline water. There are several types of renewable energy sources; the most significant of these is solar energy due to its abundance [1]. Desalination is a number of consecutive processes performed to strip all or part of the excess salts and minerals from the water. Solar stills are highly effective and straightforward devices that harness solar energy to generate freshwater without the need for multiple processes, but they employ evaporation to eliminate contaminants from water, resulting in the condensation of vapor on a glass surface within the device. The vapor is then gathered as cleansed water [2]. Solar stills can be classified into two categories: passive (direct) and active (indirect). The quality of water is very important, as it affects human health. The water industry faces a significant problem in reducing water turbidity [3]. Solar stills that are direct in nature solely depend on sunlight to promote the process of evaporation. In order to improve the evaporation process in solar stills, a range of additional components are utilized, such as phase-change materials, wick materials, solar collectors, and external condensers. Various designs, including single-slope, double-slope, spherical, and pyramid coverings, have been used to increase productivity [4], [5]. Bhargva and Yadav [6] assessed various setups, such as internal reflectors, evacuated pipe solar collectors, and external condensing systems, in order to determine the ideal water vapor temperature that would result in the most energy absorption. A comparative assessment of these improved solar stills in comparison to traditional designs demonstrated a substantially greater rate of production, reaching roughly 2300 ml/m² with an efficiency of 34% compared with traditional one-designs. Bagheri et al. [7] studied a comparison between two types of desalination processes, one with direct use of energy generated (passive), and the other with a compound parabolic collector (CPC) and solar panel for indirect usage of solar energy. Singh et al. [8]. The study conducted by Bagheri et al. [7] compared passive desalination systems with those that used a compound parabolic collector (CPC) and a solar panel to indirectly harness solar energy. Singh et al. [8] analyze the theoretical efficiency of a solar still that was equipped with evacuated tube collectors. According to the experiment, the optimal performance was achieved by employing 10 tubes and keeping the water level at 30 cm. The solar still demonstrated energy efficiencies ranging from 5.1% to 54.4% and exergy efficiencies ranging from 0.15% to 8.25%. Furthermore, the sun continued to generate a production rate of 3.6 kg/m². Patil et al. [9] addressed the critical need for fresh water in developing countries by exploring solar distillation as a viable method for desalination. The research compares four configurations of solar stills: a single slope with constant flow rate, a single slope with a secondary stepped basin, a single slope coupled with a compound parabolic concentrator, and a combination of these enhancements. The findings show that the most efficient configuration is the single slope solar still with a secondary stepped basin and compound parabolic concentrator, achieving a productivity of 1.72 kg/m² and an efficiency increase of 63.8% over the reference case. El-Sebaii et al. [10] discovered that the inclusion of phase-change materials (PCM) led to a daily efficiency of 85.3% and a production rate of 9.005 kg/m². Tanaka and Nakatake [11] enhanced the efficiency of a single-slope solar still by 48% through the utilization of both internal and external reflectors. Additionally, they achieved a 22% improvement by employing internal reflectors alone. Rajamanickam and Ragupathy [12] investigated the impact of different brine depths (10, 7.5, and 20 cm) on the efficiency of a solar still. The researchers found that the highest output of 3.07 liters per square meter was obtained when the depth of the brine was 10 centimeters. Alawee et al. [13] investigated the impact of magnetic fields on the effectiveness of solar stills in their research. They noticed significant improvements in water production, attributing it to enhanced evaporation caused by changes in the hydration shell of seawater. In an experimental investigation. Choong et al. [14] investigated the use of flat radial Fresnel lenses to enhance solar desalination by concentrating solar energy on a double-sloped solar still. Conducted in Malaysia, the research compares conventional and modified stills, using different numbers of Fresnel lenses to optimize freshwater production. Results show a 39% increase in freshwater yield with two lenses, achieving a TDS value of 37 ppm, meeting WHO standards. The study aims to optimize conditions and evaluate the effectiveness of Fresnel lenses in improving solar still performance in tropical environments. Aboud et al. [15] examined the relationship between temperature and humidity and their impact on the water output from humid air. The results indicated that as evaporation levels rise, so does the moisture content in the air. The humidity coefficient rises between 25% and 65% when the relative humidity hits 100%, leading to the condensation of water vapor, resulting in dew formation. Chaichan and Kazem [16] investigated the impact of using PCMs in a solar still and the effect of preheating the water entering the still. They employed a heat exchanger, a dish to focus sunlight, and paraffin as PCM. The trials showed that the system's efficiency improved by 180% when using a preheater without paraffin, 52% using paraffin without preheaters, and 307% using a preheater and paraffin as compared with a traditional one. Khafaji et al. [17] investigated the solar still with different depths of water. The outcomes show that with increasing water depth, the productivity decreased by about 4-9 %. The calculated values for the heat transfer coefficients through evaporation and convection were 2.62 W/m$^2$ K and 32 W/m$^2$ K, respectively, when the water depth was 1 cm. The productivity was found to be 1468.84 mL/m$^2$. The present study introduces a novel and simplified approach to enhance the productivity of solar stills by integrating a parabolic trough collector (PTC). This integration aims to address the critical research gap concerning the low efficiency of solar stills by leveraging the PTC's capability to effectively concentrate solar energy and transfer heat. The originality of this work lies in its innovative combination, which directly couples the solar still unit with a parabolic concentrator without a heat exchanger or Phase Change Material (PCM). The direct connection between the parabolic trough and the solar still helped to maximize the efficiency of the parabolic trough and eliminate losses occurring in the pipes and heat exchangers. This guarantees that more of the obtained solar energy is transferred to the water in the still, therefore generating higher temperatures and accelerating water evaporation in the solar still, which can greatly increase the yield of distilled water as compared to conventional solar. Unlike other research, which sometimes concentrates on complicated alterations or needs, this research concentrates on complicated alterations or needs, major infrastructure changes. The approach of this paper presents a pragmatic and scalable solution that can be readily applied in many environments. Both with comparable structural design, two solar stills were utilized: a Conventional Solar Still and a modified solar still that was bundled with a parabolic trough collector (PTC).

## 2. Methods and Materials

### 2.1 Experimental Work

The test system was set up at Baghdad (latitude 33.3152° N and longitude 44.3661° E). Two solar stills named CSS and MSS are constructed from 1.5 mm-thick galvanized steel plates. The solar still's low side, high side, length, and width are 12, 48, 110, and 70 cm, respectively. To close solar stills and serve as a condensing surface, a 4 mm thick glass cover was employed. The transparent cover has a transmittance of 97% allows solar energy to pass through, which is then absorbed by the water. The cover is tilted 35° to the south to capture as much solar energy as possible all year round. This absorption leads to an increase in temperature and the subsequent generation of water vapor. By natural convection, the water vapor flows towards the top transparent cover, where it condenses on the inner surface of the cover and produces freshwater that drips into the discharge channel. To avoid heat losses by convection to the atmosphere, the basins are thermally insulated on all sides with the exception of the top transparent side. Basically, the operation of solar stills is based on a distillation process and is dependent on the process of evaporation and condensation. A small inclined basin was made at the lower edge of the solar still to gather the condensation and put it into a calibrated flask.

1. The silicon substance is used to firmly seal the glass to prevent any vapor from escaping from the system. Flexible insulated pipes are used to connect the saline water tank to

the PTC, then to the modified solar still to reduce heat losses and keep the temperature of the outlet water high. The basins of both stills were installed on support structures made of 16 mm wood and 50mm thick foam sheets to insulate the sides and bottom of the stills (CSS and MSS) from the exterior in order to minimize heat losses by convection to the environment, as illustrated in Figs. 1 and 2.

2. To optimize the absorber surfaces' absorptivity, the absorption plates were painted with matte black paint. The parabolic trough is composed of two major components: the reflector and the receiver. The reflector is composed of stainless steel and has a parabolic form, with an aperture width of 80 cm and an aperture area of 1.44 $m^2$. Solar light is directed into the receiver's two-layered glass tube, which is fused at one end and has a selective absorbing coating on the outside. The outer glass tube is 183cm long, the absorber tube 5.8 cm wide, and the outer diameter 4.7 cm. In Fig. 3, the double-pass tube is welded and placed within the evacuated tube. A 0.63cm copper double-pass tube. Fiberglass closed the evacuated tube aperture, leaving only water entry holes. The rim angle of PTC is 120 °, focal distance 10 cm, receiver area 0.32 m, and concentration ratio 4. The PTC has been mounted on the wooden stand for thermal insulation of the reflector's back surface.

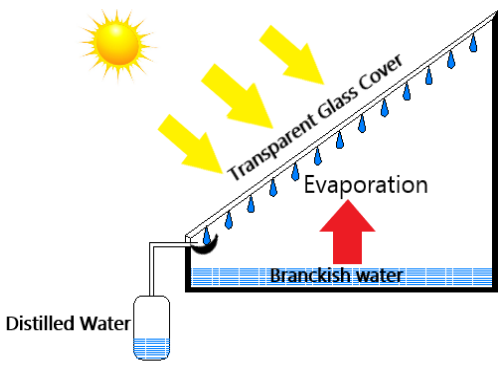


**Figure 1.** Schematic diagram of the conventional single-slope solar still.

The overall system is shown in Fig. 4. The solar radiation absorbed by the receiver tube is transferred to water flowing through the tube, which is then used to transfer the heated water to the solar still. Controlling the amount of fluid flow through the evacuated tube using a valve. K-type thermocouples were used to measure the fluid's temperature entry point into the absorbent tube and its exit point.
The schematic individual components were shown in Fig. 5

The concentration ratio of PTC was calculated from equation [18]:

$$C_r = \frac{A_a}{A_r} = \frac{W_a}{\pi d} \quad (1)$$

The efficiency of PTC is calculated from the equation below [18]:

$$\eta = \frac{mcp(T_o - T_i)}{I * A_p} \quad (2)$$

In this work, the CSS and MSS have been tested experimentally. For both solar stills, the study was divided into two cases:

- Conventional Solar Still (CSS)
- MSS with PTC with different water flow rates pumped from the water tank to PTC at four flow rates (0.001, 0.004, 0.0007, and 0.0002 kg/sec) and measure the enhancement hourly in relation to time.
- The efficiency of conventional and modified solar stills was studied.

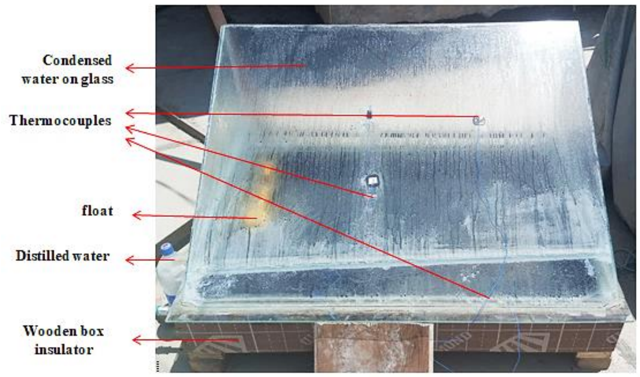


**Figure 2.** Photo of the solar still used in the experiment.

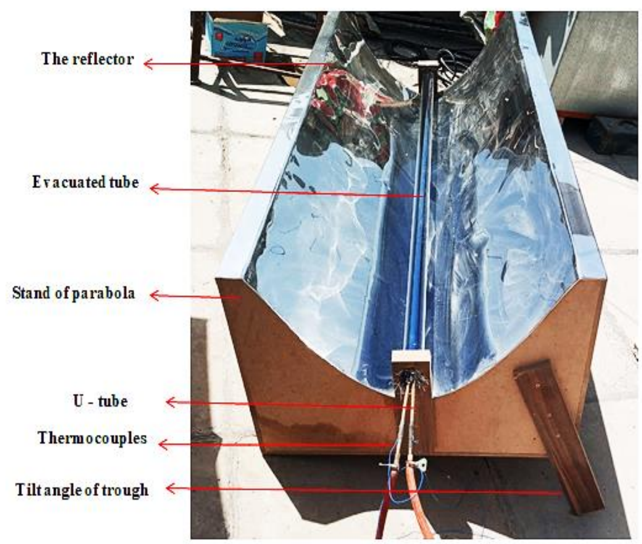


**Figure 3.** Photo of a parabolic trough collector with a double copper pipe.

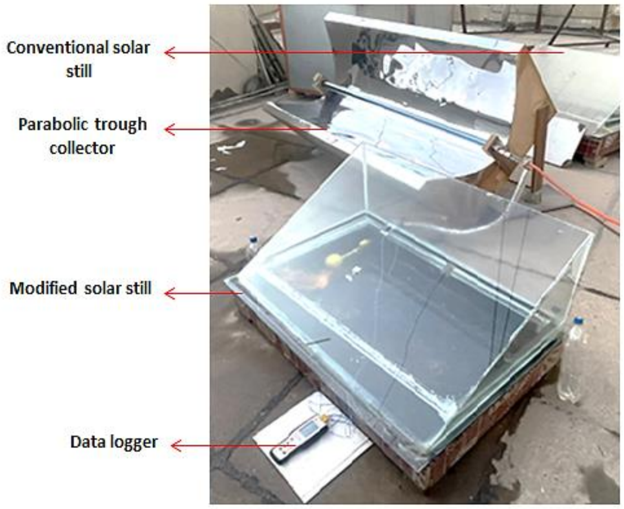


**(a)**

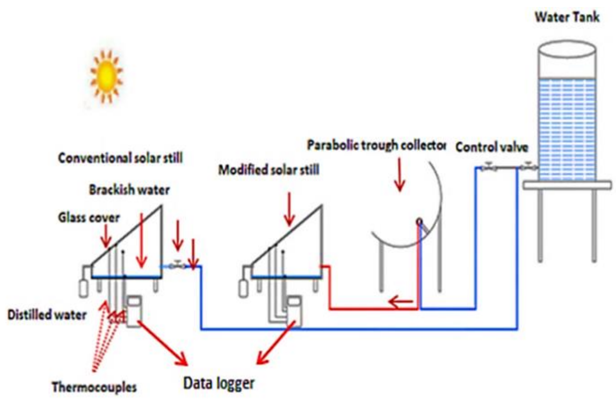


**(b)**

**Figure 4.** View of a) a photo of the overall system, b) a schematic diagram of the overall system.

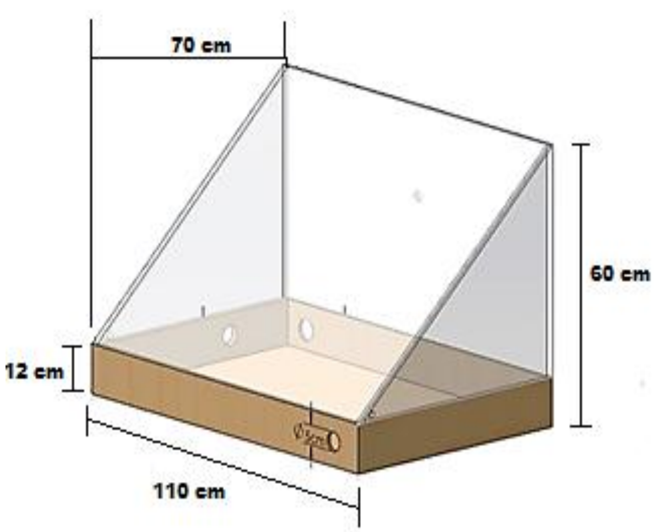


**(a)**

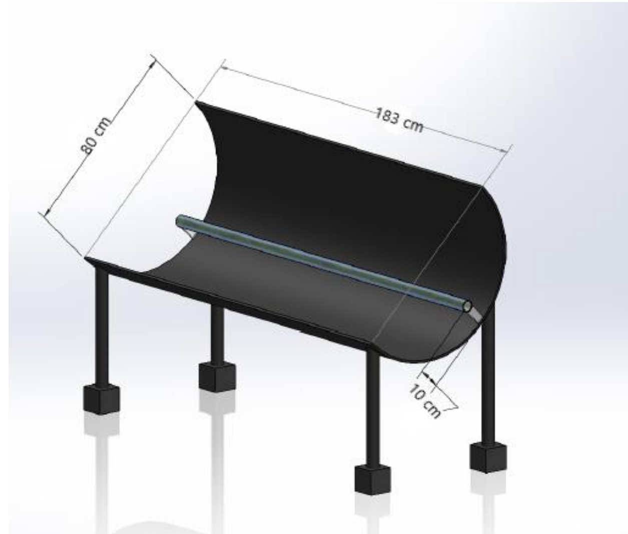


**(b)**

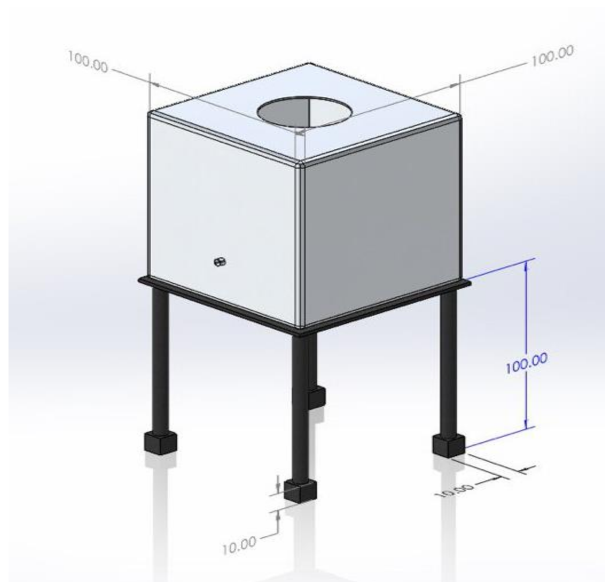


**(c)**

**Figure 5.** Schematic system components: a) solar still, b) parabolic trough reflector, c) storage tank.

### 2.2 Instrumentation

Table 1 lists the specs for the measurement equipment. K-type thermocouples (0.3 mm diameter) were utilized to measure the changes in temperature at various locations. The thermocouples were calibrated across a temperature range of 20 to 80 °C in the central organization for standardization and quality control (COSQC).

### 2.3 Experimental Measurements and Uncertainty Analysis

During every experimental measurement, the measured value often deviates from the precise value due to the inherent uncertainty in data capture. While the deviation is usually insignificant for individual variables, it can accumulate and amplify when the measured variable is used to calculate derived parameters. The accuracy of experimental measurements can be influenced by several factors that affect data precision. The main variables responsible for this issue are the imprecision of the measuring devices and the values employed in the design of the solar still and its components. Several design factors have a substantial impact on accuracy, including:

1) Thermocouples: The precision of temperature measurements relies on variables such as the kind, placement, and quantity of thermocouples employed in the experimental arrangement.
2) Fixing procedure: The way in which thermocouples are attached to the surfaces being measured can also affect the accuracy of temperature data.

**Table 1.** Technical properties of the instruments used in the work.

| NO. | Instrument | Range | Accuracy | Error |
|---|---|---|---|---|
| 1 | Thermometer | -200 °C -1370 °C | 5% | 0.36% |
| 2 | K- Type thermocouple | -50.1-200.0 °C | ±0.4%+1 °C | 0.36% |
| 3 | solar meter | 0-2000 W/m$^2$ | ±5%, ±10W/m$^2$ | 5.0% |
| 4 | anemometer | 0.4-30 m/s | ± 0.1 m/s | 1% |
| 5 | Measuring flask | 0-300 ml | ± 2 ml | 1% |
| 6 | Humidity measurement | -50-70 °C | ± 5% RH | |

It is important to assess the uncertainty in any experimental result. Various techniques can be utilized to ascertain the precision of the gathered data. The present study evaluates the uncertainty of experimental data using the methods outlined in reference [19], [20]. A set of data is examined, where the uncertainty linked to each measurement can be characterized using a coherent probability distribution. Subsequently, the desired result of the experiments is calculated using the gathered data. To estimate the uncertainties in the derived output, the errors related to the primary measurements are taken into account. $U_R$ represents the variable uncertainty, $X = X(v_1, v_2, v_3 \text{ to } v_n)$, and $U1, U2, U3$ to $Un$ present the uncertainties of the independently measured variables, has been used to estimate the uncertainties of the measured data; as shown in Table 1.

$$U_R = [\left(\frac{\partial x}{\partial v_1}U1\right)^2 + \left(\frac{\partial x}{\partial v_2}U_2\right)^2 + \left(\frac{\partial x}{\partial v_3}U_3\right)^2 + \cdots \left(\frac{\partial x}{\partial v_n}U_n\right)^2]^{\wedge}(1/2) \quad (3)$$

## 3. Results and Discussion

For the purpose of gaining helpful information and explanations on the effectiveness of the solar still, temperature measurements taken at various areas on the still are taken for four days, 13-14-15-16 August 2023. During the time span of the study, the climatic parameters, solar intensity (I), ambient temperature ($T_a$ ), wind velocity (V), and SSSS's temperatures, including water temperature , internal air temperature ($T_v$) inner cover ($T_{gi}$)outer cover temperature, water at inlet PTC, and the water at outlet PTC were measured at each one-hour interval and at different mass flow rates with the help of Type-K thermocouples. The tests lasted from 9:00 AM to 6:00 PM. All of the trials had almost identical thermal behavior of Temperatures; however, only a few were selected for graphical description.

It is obvious from Fig. 6 that the hourly variation in solar radiation refers to the changes in the solar energy received at a particular location over a day, showing a consistent increase from 8:00 to 18:00, peaking at midday between 1:00 and 1:30 PM, and tapering off in the morning and evening. Several factors influence the hourly variation of solar radiation, including the time of day, season, latitude, weather conditions, and local geographical features. Solar radiation exhibits a diurnal (daily) variation due to the rotation of the Earth, while the ambient temperature variation is also similar to the solar radiation profile. The ambient temperature initially rises and continues to rise even after the decrease in radiation. This is due to the Earth's ability to store heat; thus, as solar radiation falls, the Earth starts to release heat. Consequently, the ambient temperature remains elevated even after the sun's radiation decreases. The maximum measured ambient air temperature was 47 ◦C at 2:00 PM.

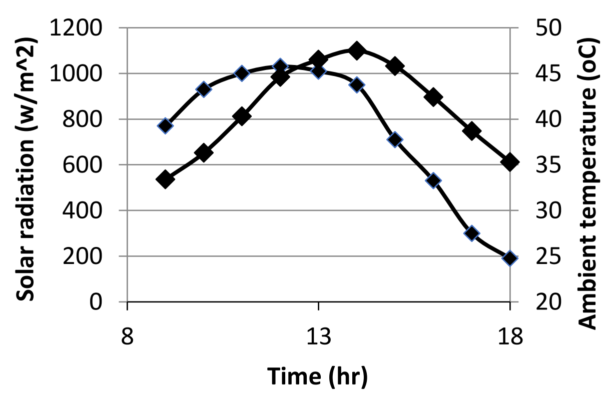


**Figure 6.** Variation of solar and ambient temperature with time.

Figs. 7, 8, and 9 illustrate the hourly temperature distributions of water, vapor, and glass. From the figures, it can be noticed that the temperatures rise until they reach their peak value at midday, then they fall as a result of the quantity of solar intensity. There is an opposite relationship between the water flow rate and the outlet water temperature from PTC. The fundamental physics explanation for this occurrence indicates that the higher flow rates reduce the time water spends in the receiver tube, leading to lower exit temperatures, while lower flow rates increase heat absorption and raise the outlet temperature. However, excessive heat can harm the system or reduce efficiency due to higher thermal losses. The water temperature peaks around midday and drops by 18:00. At a flow rate of 0.0002 kg/s, the highest water temperature reaches nearly 88.9 °C, while a flow rate of 0.0007 kg/s results in a peak of around 82.3 °C, and 0.001 kg/s yields the lowest peak temperature, slightly above 80°C.

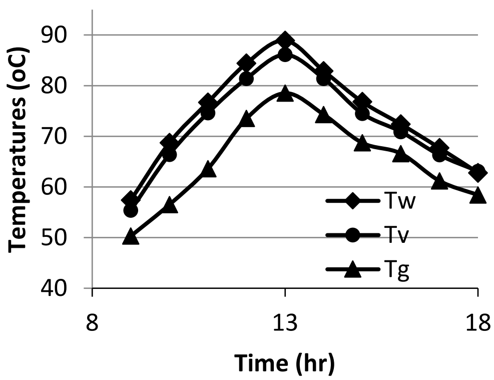


**Figure 7.** Variation of temperatures for modified solar still MSS, August 14, 2023, for flow rate 0.0002 kg/s.

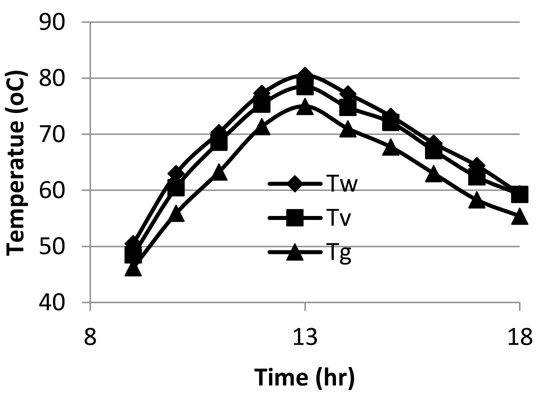


**Figure 8.** Variation of temperatures for modified solar still MSS, August 13, 2023, for flow rate 0.0007 kg/s.

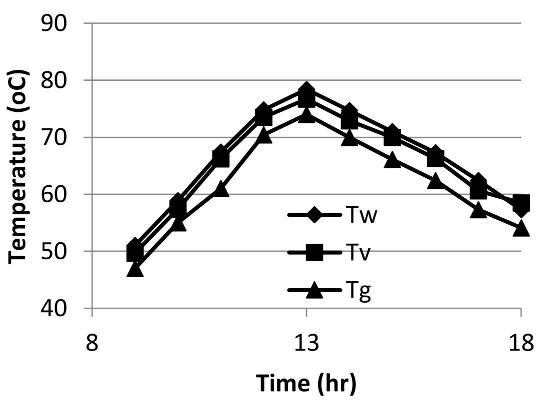


**Figure 9.** Variation of temperatures for modified solar still MSS, August 14, 2023, for flow rate 0.001 kg/s.

Raising the water flow rate in the collector generally leads to a decrease in the vapor temperature within the solar still because there exists a direct relationship between vapor temperature and water temperature; the reduction in water temperature leads to a decrease in vapor temperature accordingly. The highest vapor temperature reaches 86.4 °C, while a flow rate of 0.0007 kg/s results in a peak of around 78.8°C, and 0.001 kg/s yields the lowest peak temperature, slightly above 75 °C. Therefore, the heat transfer to the glass cover was diminished

### 3.1 The efficiency of the solar stills

The still efficiency integrated with PTC can be determined from [21], [22].

$$\eta_{still}=\frac{\sum m*h_{fg}}{A_g*I+A_c*I_c} \tag{4}$$

Fig. 10 demonstrates the hourly productivity of conventional and modified stills (at different flow rates). It highlights that the change in mass flow rate of the modified solar still has a significant effect on enhancing water productivity for the solar still. Lowering the water flow rate raises the water temperature in the solar still, enhancing evaporation and, consequently, condensation rates. This results in improved water yields, with maximum hourly distillation reaching 650 ml/m² at 13:00 = 0.0002 kg/s.

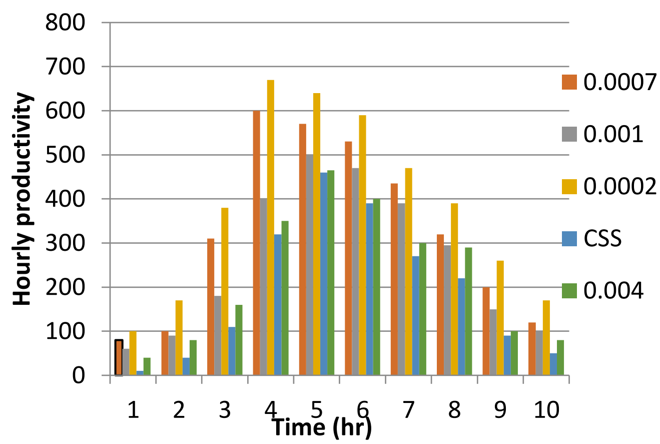


**Figure 10.** Hourly water productivity for different flow rates.

Fig. 11 represents the daily productivity of CSS was 1960 while the maximum productivity for MSS was 3840, 3265, 2635, and 2225 ml/m2 in case of flow rate 0.0002, 0.0007, 0.001, and 0.004 kg/s, respectively. So, the enhancement ratio is 95.81%, 66.5%, 28.85%, 34.4% at flow rates of 0.0002, 0.0007, 0.001, and 0.004 kg/s, respectively, over CSS.

Fig. 12 represents the efficiency of still, which is equal to the distillate of a certain volume of salt water to the available solar intensity at that time. When the productivity increased, the efficiency increased due to the linear relation between them.

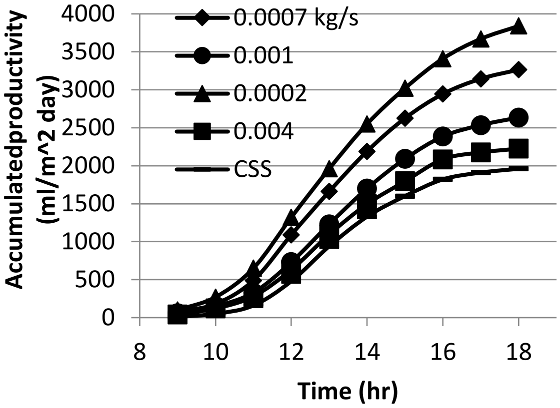


**Figure 11.** Accumulated productivity for all cases.

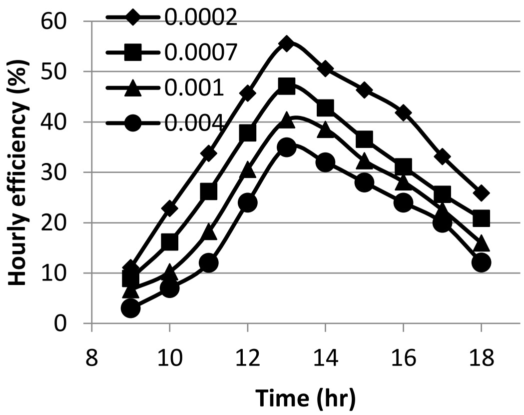


**Figure 12.** Daily efficiency for all cases.

An analysis of the findings from this study in relation to other similar investigations is listed in Table 2. The performance of the single slope solar still was significantly improved with this improvement, surpassing the results of previous researchers**.**

**Table 2.** Comparison between the current study and similar studies.

| No. | Researcher | Improvement method | Increase in production % |
|---|---|---|---|
| 1 | Hameed et al. [21] | absorbent base with various stainless-steel geometries | 38.2% |
| 2 | Patil et al. [9] | Applied an evacuated tube to increase the incident solar radiation on the solar still | 63.8% |
| 3 | Choong et al. [14] | Used Fresnel lenses to concentrate solar energy onto the still's surface. | Achieved a 39% increase in productivity compared to a conventional solar still. |
| 4 | Singh et al. [8] | Solar still with evacuated Tube | 33% |
| 5 | Present Study | Solar still with PTC at different flow rates | 13.5-95.8% depend on mass flow rate |

### 3.2 Economic cost

The major items of annual costs are the component's capital cost. The total cost can be obtained by summing fixed and variable costs as follows:

$$V_c = 0.3\ F_c * n \qquad (5)\ [21]$$

**I. Case 1, CSS**

The fixed cost of CSS is about F = $80. To determine the average cost of distillate output, the following hypotheses are developed in order to calculate the average cost of distillate output: V is the variable cost, and n is the expected still life.

$V = 0.3\ F_c * n$ , $C_t$Is the total cost equal to:

$$C_t = F_c + V_c \qquad (6)$$

The expected still life is 10 years, then, Ct = 80 + (0.3*80*10) = $ 320, the minimal average daily productivity can be derived from the previous data, and it's assumed that 2.2 $l/m^2$ per day. Assume that they still operate 270 days a year. The total productivity during the still life = 5940 liters. Cost per liter from conventional still= 0.053 $/l.

**II. Case 2, MSS**

The fixed cost of MSS is about F = $ 100 with PTC. Assume it will still be operating for ten years. The variable cost = (100*0.3*10) = $ 300, Ct= 400$. The minimum average daily yield can be derived from the previous data and is assumed to be 3.840 L/m2 per day. The overall production in still life = 10368 liters. Cost per liter = 0.038 $/l.

## 4. Conclusions

The following conclusions have been reached based on experimental data of the design of a single slope solar still combined with PTC in Baghdad climate conditions. The results demonstrated that incorporating PTC into the still may improve the solar still's output by 13.5%, 34.3%, 66.5% and 95.8% at mass flow rates of 0.004, 0.001, 0.0007, and 0.0002 kg/s, respectively, on August 14, 15, 16, and 17, of August 2023. Also, the basin water's temperature at 2:00 PM is 69. °C, 71.2°C, 74.7°C, 77.2°C, 82.9°C for CSS and MSS (0.004, 0.001, 0.0007, 0.0002 kg/s) respectively, due to the added heat source (the parabolic trough collector). These temperatures decreased slowly at 18 PM. The efficiency of each flow rate of the modified solar still increased with an increase in mass flow rate, where the maximum efficiency at 1 PM is 58%, 46.7 %, 40%, 35% at 0.004, 0.001, 0.0007, 0.0002 kg/s, respectively. The economic feasibility of this study was studied, and it was found that the cost of portable water is about 0.038 $/l by the present modified solar still compared with 0.053 $/l for a conventional solar still.

## List of Symbols

| | |
|---|---|
| Aa | Aperture Area ($m^2$) |
| Ar | Receiver Area ($m^2$) |
| Aa | Apparent area ($m^2$) |
| $h_{fg}$ | Latent heat of vaporization (J/kg) |
| I | Solar radiation ($W/m^2$) |
| $\dot{m}$ | mass flow rate ($m^3/s$) |
| $m_d$ | Hourly productivity ($kg/m^2$) |
| $T_w$ | Water Temperature (°C) |
| $T_g$ | Glass Temperature (°C) |
| $T_v$ | Vapor Temperature (°C) |
| $T_a$ | Ambient Temperature (°C) |
| Wa | Aperture width (m) |
| Ag | glass Area ($m^2$) |
| Ac | Collector area ($m^2$) |
| $\emptyset_r$ | Rim angle |

## List of Abbreviations

| | |
|---|---|
| CSS | Conventional Solar Stills |
| SD | Solar Distillation |
| PTC | Parabolic Trough Collector |
| MSS | Modified Solar Still |
| SSSS | Single Slope Solar Still |

## Subscript

| | |
|---|---|
| amb | ambient |
| a | aperture |
| g | Glass |
| w | water |
| c | cost |
| e | evaporation |
| o | outer |
| i | inner |
| abs | absorber |
| ref | reflector |

## Acknowledgements

The authors acknowledge the University of Technology, Iraq, and the reviewers for their insightful comments.

## Author Contribution Statement

Lujain S. Hyal, Jalal M. Jalil, and Abduljabbar O. Hanfesh proposed the research problem, developed the theory, and performed the computations.
Jalal M. Jalil, Abduljabbar O. Hanfesh verified the analytical methods, investigated, and supervised the findings of this work. All authors discussed the results and contributed to the final manuscript.

## Declaration of Competing Interest

The authors declare that they have no known competing financial interests or personal relationships that could have appeared to influence the work reported in this paper.

## References

[1] S. H. Ahmed, A. K. Ibrahim, and M. F. Abed, "Assessing the quality of the groundwater and the nitrate exposure, North Salah Al-Din Governorate, Iraq: Quality of groundwater," *Tikrit Journal of Engineering Sciences*, vol. 30, no. 1, pp. 25–36, 2023. doi: https://doi.org/10.25130/tjes.30.1.3.

[2] A. M. Kadhum, M. H. Al-Furaiji, and Z. N. Abudi, "Evaluation of thin film composite forward osmosis membranes: Effect of polymer type," Journal of Engineering and Sustainable Development, vol. 25, no. 6, pp. 65–73, 2021. doi: https://doi.org/10.31272/jeasd.25.6.7.

[3] Z. H. Abed and K. M. Khudair, "Modeling of Turbidity Distribution in Water Networks Using PMS Model-Al-Saray Sector in Kufa City As a Case Study," *Kufa Journal of Engineering*, vol. 14, no. 3, pp. 48–68, 2023. doi: https://doi.org/10.30572/2018/KJE/140304.

[4] M. A. Salih and A. H. Dhiaa, "Performance Evaluation of the Reverse Osmosis Pilot Plant: Using Sodium Chloride and Magnesium Chloride," *Kufa Journal of Engineering*, vol. 14, no. 2, pp. 1–11, 2023. doi: https://doi.org/10.30572/2018/KJE/140201.

[5] M. Fathy, H. Hassan, and M. S. Ahmed, "Experimental study on the effect of coupling a parabolic trough collector with a double slope solar still on its performance," *Solar Energy*, vol. 163, pp. 54–61, 2018. doi: https://doi.org/10.1016/j.solener.2018.01.043.

[6] M. Bhargva and A. Yadav, "Effect of shading and evaporative cooling of glass cover on the performance of evacuated tube-augmented solar still," *Environment, Development and Sustainability*, vol. 22, pp. 4125–4143, 2020. doi: https://doi.org/10.1007/s10668-019-00375-8.

[7] A. Bagheri, N. Esfandiari, B. Honarvar, and A. Azdarpour, "ANN Modeling and experimental study of the effect of various factors on solar desalination," *Water Supply*, vol. 20, no. 1, pp. 259–268, 2020. doi: https://doi.org/10.2166/aqua.2020.085.

[8] R. V. Singh, S. Kumar, M. M. Hasan, M. E. Khan, and G. N. Tiwari, "Performance of a solar still integrated with evacuated tube collector in natural mode," *Desalination*, vol. 318, pp. 25–33, 2013. doi: https://doi.org/10.1016/j.desal.2013.03.012.

[9] B. Patil, J. Hole, and S. Wankhede, "Performance enhancement of stepped solar still coupled with evacuated tube collector," *Journal of Thermal Engineering*, vol. 9, no. 5, pp. 1177–1188, 2023. doi: https://doi.org/10.18186/thermal.1372168.

[10] A. A. El-Sebaii, A. A. Al-Ghamdi, F. S. Al-Hazmi, and A. S. Faidah, "Thermal performance of a single basin solar still with PCM as a storage medium," *Applied Energy*, vol. 86, no. 7–8, pp. 1187–1195, 2009. doi: https://doi.org/10.1016/j.apenergy.2008.10.014.

[11] H. Tanaka and Y. Nakatake, "Theoretical analysis of a basin type solar still with internal and external reflectors," *Desalination*, vol. 197, no. 1–3, pp. 205–216, 2006. doi: https://doi.org/10.1016/j.desal.2006.01.017.

[12] M. R. Rajamanickam and A. Ragupathy, "Influence of water depth on internal heat and mass transfer in a double slope solar still," *Energy Procedia*, vol. 14, pp. 1701–1708, 2012. doi: https://doi.org/10.1016/j.egypro.2011.12.1155 .

[13] W. H. Alawee et al., "Effects of magnetic field on the performance of solar distillers: A review study," *Engineering and Technology Journal*, vol. 41, no. 1, pp. 121–131, 2023. doi: https://doi.org/10.30684/etj.2022.134576.1240.

[14] W. S. Choong, Z. Y. Ho, and R. Bahar, "Solar desalination using Fresnel lens as concentrated solar power device: An experimental study in tropical climate," *Frontiers in Energy Research*, vol. 8, p. 565542, 2020. doi: https://doi.org/10.3389/fenrg.2020.565542.

[15] G. A. Aboud, H. A. Hussein, and A. H. Numan, "Effect of Temperature and Humidity Factors on Water Production Using Solar Energy with Smart Controlling," *Engineering and Technology Journal*, vol. 40, no. 1, pp. 241–248, 2022. doi: https://doi.org/10.30684/etj.v40i1.2282.

[16] M. T. Chaichan and H. A. Kazem, "Water solar distiller productivity enhancement using concentrating solar water heater and phase change

material (PCM)," *Case Studies in Thermal Engineering*, vol. 5, pp. 151–159, 2015. doi: https://doi.org/10.1016/j.csite.2015.03.009.

[17] H. Q. A. Khafaji, H. A. Abdul Wahhab, W. A. K. Al-Maliki, F. Alobaid, and B. Epple, "Energy and exergy analysis for single slope passive solar still with different water depth located in Baghdad center," *Applied Sciences*, vol. 12, no. 17, p. 8561, 2022. doi: https://doi.org/10.3390/app12178561.

[18] H. J. Jaber, Q. A. Rishak, and Q. A. Abed, "Using PCM, an Experimental Study on Solar Stills Coupled with and without a Parabolic Trough Solar Collector," *Basrah Journal for Engineering Sciences*, vol. 21, no. 2, pp. 45–52, 2021. doi: https://doi.org/10.33971/bjes.21.2.7.

[19] R. J. Moffat, "Describing the uncertainties in experimental results," *Experimental Thermal and Fluid Science*, vol. 1, no. 1, pp. 3–17, 1988. doi: https://doi.org/10.1016/0894-1777(88)90043-X.

[20] J. Holman, Experimental Methods for Engineers, 8th ed. New York, NY, USA: McGraw-Hill, 2012.

[21] H. G. Hameed, H. A. N. Diabil, and M. A. Al-Moussawi, "A numerical investigation of the enhancement of single-slope single-basin solar still productivity," *Energy Reports*, vol. 9, pp. 484–500, 2023. doi: https://doi.org/10.1016/j.egyr.2022.11.199.

[22] K. Sampathkumar and P. Senthilkumar, "Utilization of solar water heater in a single basin solar still—an experimental study," *Desalination*, vol. 297, pp. 8–19, 2012. doi: https://doi.org/10.1016/j.desal.2012.04.012.